Polarization observables and spin-aligned fusion rates in ^{2}H$(d,p)^3$H and ^{2}H$(d,n)^3$He reactions

A. Deltuva* and A. C. Fonseca
Centro de Física Nuclear da Universidade de Lisboa, P-1649-003 Lisboa, Portugal
(Received 24 February 2010; published 24 May 2010)

Nucleon transfer reactions in low-energy deuteron-deuteron scattering are described by solving exact four-particle equations in momentum space. The Coulomb interaction between the protons is included using the screening and renormalization method. Various realistic potentials are used between nucleon pairs. The energy dependence of the differential cross section, analyzing powers, polarizations, spin-transfer coefficient, and the quintet suppression factor is studied.

DOI: 10.1103/PhysRevC.81.054002 PACS number(s): 21.30.−x, 21.45.−v, 24.70.+s, 25.10.+s

I. INTRODUCTION

Neutron (n) and proton (p) transfer reactions in deuteron-deuteron (d-d) scattering, $d + d \to p + {}^3$H and $d + d \to n + {}^3$He, are among the simplest nuclear reactions where charge-symmetry breaking (CSB) in the nuclear force can be verified or searched for. For that purpose one needs a very precise calculation of the four-nucleon ($4N$) problem with different interaction models based on nucleon-nucleon (NN) and many-nucleon forces, together with the inclusion of the Coulomb force between protons, which is the most important cause of CSB. Such a task is now possible in view of the progress achieved in the past few years [1,2] on the solution of exact Alt, Grassberger, and Sandhas (AGS) equations [3] for four-particle transitions operators that, in addition to the strong nuclear force, include also the Coulomb interaction.

The aim of the present article is to study the energy dependence of the $d + d \to p + {}^3$H and $d + d \to n + {}^3$He observables below the three-body breakup threshold using different nuclear force models. In addition to the differential cross sections [4–7], there are precise measurements of the deuteron analyzing powers between 1.5- and 4-MeV deuteron laboratory energy [6,8]. The analyzing powers show a complex structure of maxima and minima that in some cases varies rapidly with the energy. These rapid variations and complex structure mean that different dd partial waves play a significant role, and agreement or disagreement with experimental data at different energies may result from a delicate interplay between them. The contribution of each partial wave to the observables and their evolution with the energy is analyzed.

Other observables that were measured but never analyzed through exact $4N$ calculations are polarization of the outgoing nucleon [9] and deuteron-to-nucleon spin-transfer coefficients [10,11]; they are also calculated in the present work.

Furthermore, we will get back to an old issue that remains of interest in d-d fusion in hot plasma. It was initially believed [12] that at very low energy the production of neutrons resulting from $d + d \to n + {}^3$He could be controlled by polarizing all deuterons in the plasma such that only spin-aligned d-d fusion would take place. If spin-aligned $d + d \to n + {}^3$He reaction would be significantly suppressed compared to $d + d \to p + {}^3$H, one would have a significant reduction of undesired neutrons coming out of the plasma. In the past, many approximate calculations were made that yielded contradicting results. More sophisticated calculations [13] indicated that no strong suppression should be expected. The present well-converged $4N$ calculations aim at settling the assumption in the possible suppression of $d + d \to n + {}^3$He reaction with spin-aligned deuterons.

II. RESULTS

Our description of the $4N$ system is based on exact four-particle equations for the transition operators as derived by Alt, Grassberger, and Sandhas [3]; they are equivalent to the Faddeev-Yakubovsky equations [14] for the wave-function components. Because in the isospin formalism protons and neutrons can be considered as identical particles, the symmetrized form of the AGS equations [1,2] is appropriate. Although the initial d-d state has total isospin $\mathcal{T} = 0$, the final n-^{3}He and p-^{3}H states are dominated by both isospin $\mathcal{T} = 0$ and $\mathcal{T} = 1$ components; a very small admixture of $\mathcal{T} = 2$ is present owing to the charge dependence of the hadronic and electromagnetic interactions. The most important source for the total isospin nonconservation is the Coulomb force between the protons; it is included using the method of screening and renormalization [15–18]. The hadronic charge dependence, as given by the modern NN potentials, is taken into account as well. After partial wave decomposition, the AGS equations are a system of three-variable integral equations that are solved numerically without any approximation beyond the usual discretization of momentum variables on a finite mesh; technical details are given in Refs. [1,2]. The results we present are well converged with respect to the partial-wave expansion, the number of momentum mesh points, and the Coulomb screening radius used to calculate the short-range part of the amplitudes. In this way the discrepancies with the experimental data may be attributed solely to the underlying NN forces or the lack of many-nucleon forces.

As two-nucleon interactions we use the phenomenological potentials Argonne V18 (AV18, hadronic part only) [19] and charge-dependent Bonn (CD Bonn) [20], inside nonlocal outside Yukawa (INOY04) potential by Doleschall [21], and the one derived from the chiral perturbation theory at next-to-next-to-next-to-leading order (N3LO) [22]. Furthermore, we consider also a two-baryon coupled-channel potential including virtual excitation of a nucleon to a Δ isobar [23]

*deltuva@cii.fc.ul.pt

TABLE I. ^{3}H and ^{3}He binding energies (in MeV) and deuteron D-state probability $P_D(d)$ (in percent) for different NN potentials.

	$B\,(^3\mathrm{H})$	$B\,(^3\mathrm{He})$	$P_D\,(d)$
AV18	7.66	6.95	5.78
N3LO	7.85	7.13	4.51
CD Bonn	8.00	7.26	4.85
CD Bonn + Δ	8.28	7.53	4.85
INOY04	8.49	7.73	3.60
Experiment	8.48	7.72	

that in the 4N system yields effective 3N and 4N forces [24]. Point Coulomb is added for pp pairs. ^{3}He and ^{3}H binding energies calculated with those potentials are collected in the Table I. Thus, the presence of the 3N force is also simulated by the potential INOY04 that fits both ^{3}He and ^{3}H experimental binding energies and thereby of all the used potentials is the only one that reproduces correctly the momenta of the final n-^{3}He and p-^{3}H states. For this reason it is not surprising to see that INOY04 potential gives the best description of $d + d \to n + {}^3$He and $d + d \to p + {}^3$H data. We therefore show the predictions of all potentials for the reactions at deuteron laboratory energy $E_d = 3$ MeV but study the energy dependence of the observables using INOY04 only.

Although d-d elastic scattering is calculated simultaneously with the transfer reactions, it is a less interesting case and therefore not discussed in the present work: As demonstrated in Refs. [2,24], the d-d elastic cross section data is well described by all NN force models and the corresponding

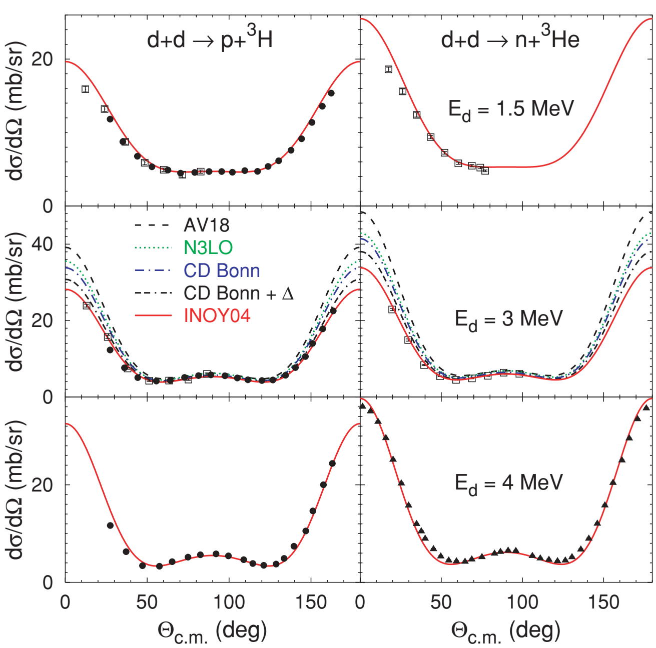

FIG. 1. (Color online) Differential cross sections of $d + d \to p + {}^3$H and $d + d \to n + {}^3$He reactions at 1.5-, 3-, and 4-MeV deuteron laboratory energy as functions of the nucleon c.m. scattering angle. Results obtained with various realistic NN potentials are compared with the experimental data from Refs. [4] (squares), [6,7] (circles), and [5] (triangles); the latter set is taken at $E_d = 3.7$ MeV.

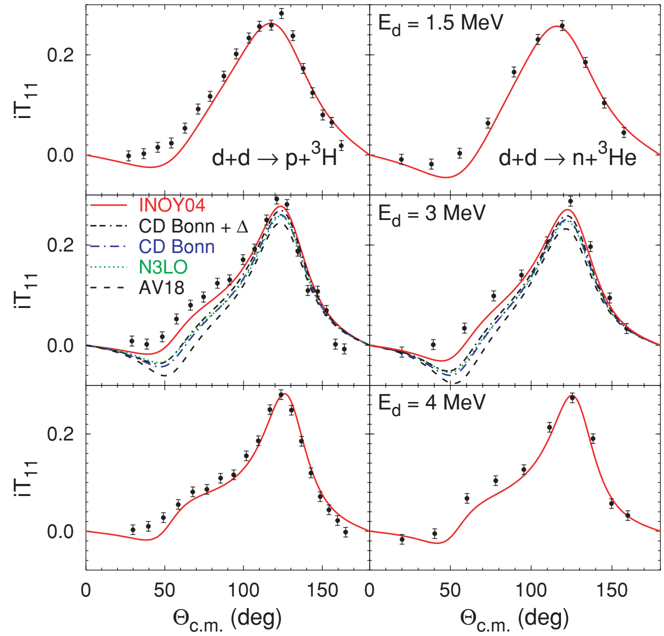

FIG. 2. (Color online) Deuteron vector analyzing power iT_{11} of $d + d \to p + {}^3$H and $d + d \to n + {}^3$He reactions at 1.5-, 3-, and 4-MeV deuteron laboratory energy. The data are from Refs. [6,7] for $d + d \to p + {}^3$H and Ref. [8] for $d + d \to n + {}^3$He.

deuteron analyzing powers are very small with quite large error bars that preclude physics conclusions.

In Fig. 1 we present the differential cross section $d\sigma/d\Omega$ results for both $d + d \to p + {}^3$H and $d + d \to n + {}^3$He reactions at $E_d = 1.5$, 3, and 4 MeV as function of the nucleon center-of-mass (c.m.) scattering angle $\Theta_{\mathrm{c.m.}}$. This observable is symmetric with respect to $\Theta_{\mathrm{c.m.}} = 90^\circ$. While at the lowest energy the differential cross section is flat between $\Theta_{\mathrm{c.m.}} = 60^\circ$ and 120°, with increasing energy it develops a minima around $\Theta_{\mathrm{c.m.}} = 55^\circ$ and 125° and a local maximum at $\Theta_{\mathrm{c.m.}} = 90^\circ$. Furthermore, $d\sigma/d\Omega$ increases with energy at forward and backward angles. There is a good agreement between the experimental data and the predictions of the INOY04 potential, whereas other models overestimate the data, especially at forward and backward angles; furthermore, the discrepancy seems to be proportional to the defect in theoretical ^{3}He and ^{3}H binding energies. Thus, the differential cross section in the considered transfer reactions correlates nearly linearly with 3N binding energies.

In Figs. 2–5 we present the corresponding results for the deuteron analyzing powers. The vector analyzing power iT_{11} in Fig. 2 varies quite slowly with the energy. The experimental data are well reproduced by the INOY04 model, although a small discrepancy remains around $\Theta_{\mathrm{c.m.}} = 45^\circ$. More significant discrepancies take place in the tensor analyzing power T_{20} (Fig. 3) at small scattering angles, although this observable is slightly overestimated in almost the whole kinematical regime. Nevertheless, the energy dependence of T_{20}, being considerably stronger than for iT_{11}, is well reproduced by the calculations. The tensor analyzing power T_{21} (Fig. 4), though showing strong energy dependence at intermediate angles, is quite well accounted for by the INOY04 predictions. The description of

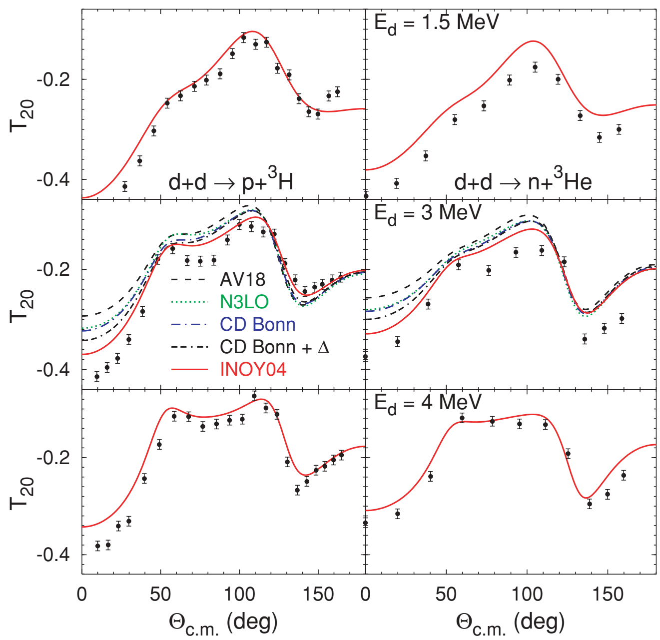

FIG. 3. (Color online) Same as Fig. 2 but for the deuteron tensor analyzing power T_{20}.

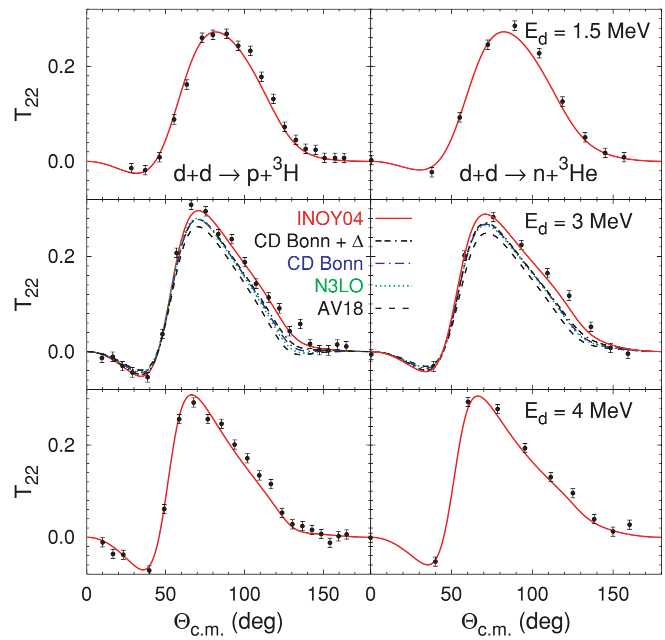

FIG. 5. (Color online) Same as Fig. 2 but for the deuteron tensor analyzing power T_{22}.

the tensor analyzing power T_{22} (Fig. 5) is even better; this observable, much like iT_{11}, varies slowly with the energy. The results obtained with other NN potentials at $E_d = 3$ MeV deviate from the respective data more significantly. Furthermore, even if the reproduction of experimental binding energies is an important factor, it is certainly not the only one that matters because the linear correlation with $3N$ binding energies seems to be violated, for example, for iT_{11} at $\Theta_{\text{c.m.}}$ between 40° and 90° or for T_{22} between $\Theta_{\text{c.m.}} = 60°$ and 120°, the predictions of N3LO, CD Bonn, and CD Bonn + Δ almost coincide despite quite significant differences (up to 0.4 MeV) in the respective $3N$ binding energies, while the predictions of INOY04 and AV18 stay well separated. A closer look into the calculated properties of deuteron, ^{3}He, and ^{3}H as given in Table I suggests that the considered spin observables correlate, in addition to the $3N$ binding energy, also with the D-state probability of deuteron $P_D(d)$. The correlation between $P_D(d)$ and $3N$ binding energy takes place for most phenomenological NN potentials, but N3LO and CD Bonn + Δ models clearly violate that correlation, thereby making it possible to study the dependence of $4N$ observables on both $3N$ binding energy and $P_D(d)$. The results in Figs. 2–5 indicate that increasing the $3N$ binding energy and decreasing $P_D(d)$ move the theoretical predictions into the same direction but the corresponding rates, that is, strength of the correlations, depend on the observable and kinematical regimes. One may conjecture that by a slight decrease in $P_D(d)$ of INOY04, while keeping the ^{3}He and ^{3}H binding energies unchanged, one might be able to cure the iT_{11} discrepancy around $\Theta_{\text{c.m.}} = 45°$. However, T_{20} shows quite weak correlation with $P_D(d)$ and therefore its description would not be improved significantly by a small decrease in $P_D(d)$.

In Fig. 6 we present the results for the polarization P_y of the outgoing nucleon in $d + d \to p + {}^3$H and $d + d \to n + {}^3$He reactions; this observable is equivalent to the nucleon-analyzing power A_y in the time-reverse reactions $p + {}^3$H $\to d + d$ and $n + {}^3$He $\to d + d$. P_y is antisymmetric with respect to $\Theta_{\text{c.m.}} = 90°$; we therefore show only the angular regime up to $\Theta_{\text{c.m.}} = 90°$, which contains all the available data. P_y shows quite strong energy dependence; in the $d + d \to p + {}^3$H case it even changes the sign when E_d varies from 2 to 4 MeV, being almost zero at $E_d = 3$ MeV. In the $d + d \to n + {}^3$He case the observable changes with the same trend but with about a 1.5-MeV shift in the energy. The qualitative reproduction of

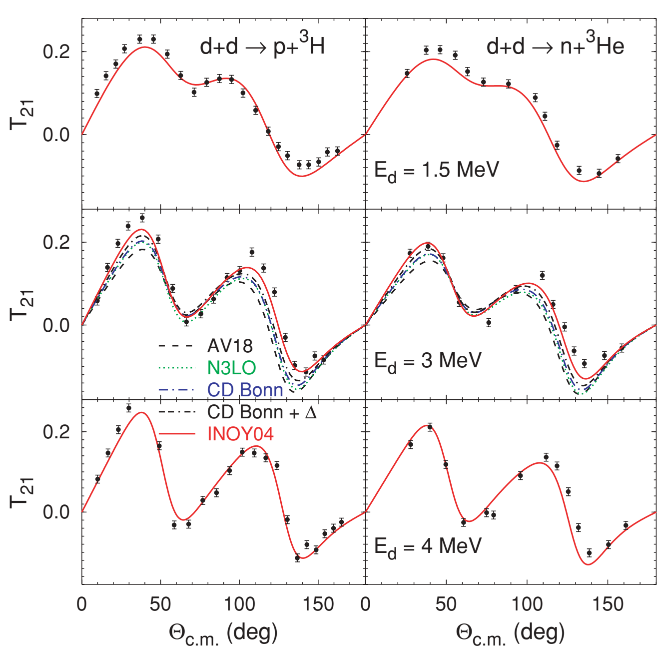

FIG. 4. (Color online) Same as Fig. 2 but for the deuteron tensor analyzing power T_{21}.

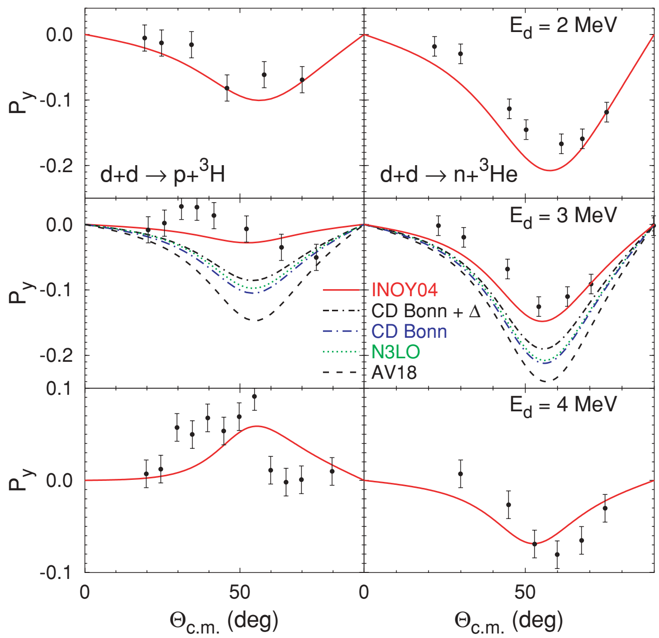

FIG. 6. (Color online) Outgoing nucleon polarization P_y of $d + d \to p + {}^3\mathrm{H}$ and $d + d \to n + {}^3\mathrm{He}$ reactions at 2-, 3-, and 4-MeV deuteron laboratory energy. The data are from Ref. [9].

the experimental data having large error bars is quite successful using the potential INOY04, whereas predictions using the other interaction models are further away. As the deuteron-analyzing powers, the nucleon polarization correlates not only with the $3N$ binding energy but also with $P_D(d)$, as one can see by comparing N3LO, CD Bonn, and CD Bonn + Δ results.

Next we consider double-polarization observables for which, unfortunately, the experimental data are much scarcer. The deuteron-to-neutron spin-transfer coefficient K_y^y has been measured in several experiments [10,11], however, only for the neutrons emitted in the forward direction $\Theta_{\mathrm{c.m.}} = 0°$; the data for the corresponding observable in the $d + d \to p + {}^3\mathrm{H}$ reaction are not available below the three-body breakup threshold. In Fig. 7 we compare the deuteron-to-neutron spin-transfer coefficient $K_y^y(0°)$ calculated using the INOY04 potential with two sets of experimental data in the energy range $0.75 \leqslant E_d \leqslant 4$ MeV. There is a good agreement above $E_d = 2$ MeV, while at lower energies, where the observable shows stronger energy dependence, the data points from Ref. [11] are slightly overpredicted. We include in Fig. 7 also the calculated $K_y^y(0°)$ for the $d + d \to p + {}^3\mathrm{H}$ reaction that shows a similar behavior. The dependence on the NN force model is quite weak for $K_y^y(0°)$, considerably smaller than the experimental error bars: At $E_d = 3$ MeV the predictions of AV18, N3LO, CD Bonn, CD Bonn + Δ, and INOY04 are 0.622, 0.626, 0.630, 0.632, and 0.633, respectively.

In Fig. 8 we study the contribution of various initial and final-state partial waves characterized by the relative

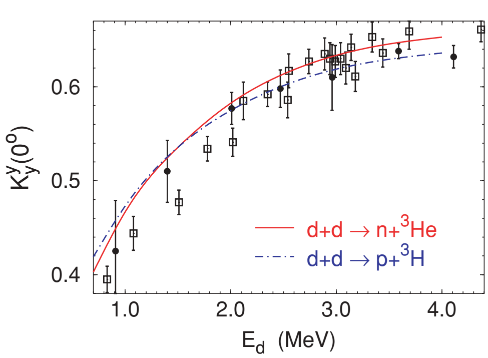

FIG. 7. (Color online) Deuteron to nucleon spin transfer coefficient K_y^y for $d + d \to p + {}^3\mathrm{H}$ and $d + d \to n + {}^3\mathrm{He}$ reactions at $\Theta_{\mathrm{c.m.}} = 0°$ as function of the deuteron laboratory energy. The data are from Ref. [10] (circles) and from Ref. [11] (squares); both sets refer to the $d + d \to n + {}^3\mathrm{He}$ reaction.

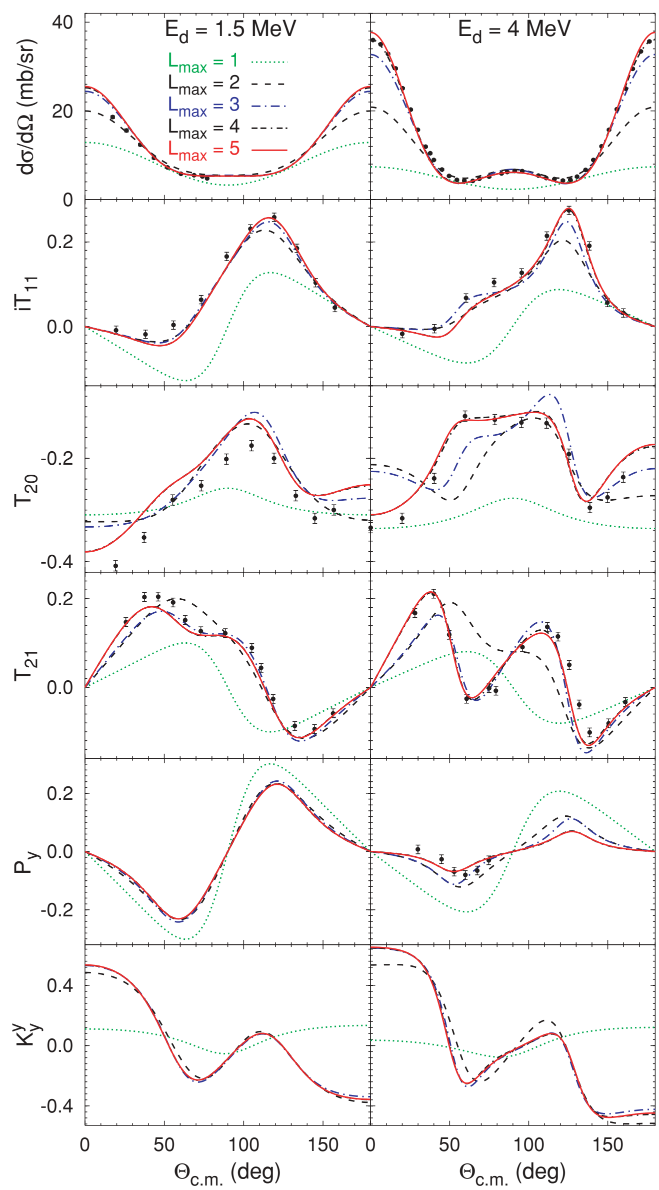

FIG. 8. (Color online) Observables of $d + d \to n + {}^3\mathrm{He}$ reaction at $E_d = 1.5$ and 4 MeV. Results including initial and final states with two-cluster relative orbital angular momentum $L \leqslant L_{\max}$ are compared for $L_{\max}$ ranging from 1 to 5. $L_{\max} = 4$ and 5 results lie almost on top of each other. The experimental data are as in previous figures.

two-cluster (i.e., d-d, n-^{3}He, and p-^{3}H) orbital angular momentum L. Because $d + d \to p + {}^3$H and $d + d \to n + {}^3$He observables show similar behavior, we restrict our study to the latter reaction at $E_d = 1.5$ and 4 MeV. We performed a series of calculations with INOY04 potential, including $L \leqslant L_{\max}$ with $L_{\max}$ ranging from 1 to 5. The predictions with $L_{\max} = 4$ and 5 are very close, indicating that the $L = 5$ contribution is very small; however, because the convergence is not monotonic, we have also verified that the $L = 6$ contribution can be safely neglected. In contrast, the partial waves with $L = 4$ yield a sizable contribution at $E_d = 4$ MeV and for the deuteron-tensor-analyzing powers even at $E_d = 1.5$ MeV. For other observables at this energy $L_{\max} = 3$ is sufficient, while P_y is reasonably well converged with $L_{\max} = 2$. It is interesting to note that $L_{\max} = 1$ results for most observables vary slowly with the energy while stronger energy dependence comes from $L = 2$, 3, and 4 partial waves. The above analysis partially explains sizable differences between our converged results and those of Ref. [25] obtained using the resonanting group method (RGM) because the latter work included only $L \leqslant 3$ states. Our AV18 results calculated with $L_{\max} = 3$ (not shown here) are qualitatively similar to the corresponding results of Ref. [25].

Finally, we present results for the observables characterizing the spin correlations of the initial-state deuterons. We are not aware of the existence of experimental data, but there are plans [26,27] for future experiments involving the direct measurement of the so-called quintet suppression factor (QSF), defined as the ratio σ_2/σ, where σ_2 is the cross section for the considered transfer reaction with the spins of the initial-state deuterons being parallel, that is, with the total spin being 2, and σ is the unpolarized (spin-averaged) cross section. As mentioned in the Introduction, this observable is relevant for d-d fusion in hot plasma. Results obtained using INOY04 potential for E_d between 50 keV and 4 MeV are shown in Fig. 9. The QSF for the $d + d \to n + {}^3$He reaction is indeed smaller than for $d + d \to p + {}^3$H; however, the difference is only about 20%–25% in the whole considered regime. The energy dependence of the QSF is in both reactions similar: It is of the order of 0.25 above $E_d = 2$ MeV but increases more rapidly as the energy decreases. Nevertheless, our QSF prediction is somehow smaller than the values obtained from R-matrix analysis and RGM [13]. This observable shows also

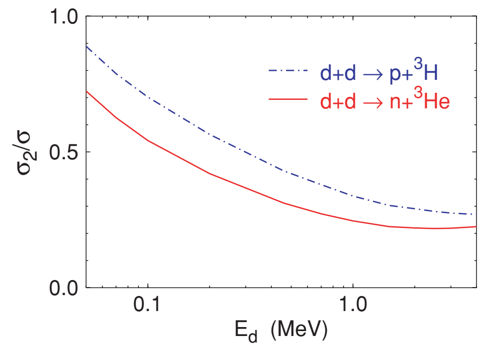

FIG. 9. (Color online) The quintet suppression factor σ_2/σ for $d + d \to p + {}^3$H and $d + d \to n + {}^3$He reactions as a function of the deuteron laboratory energy.

strong dependence on the NN force model; for example, the QSF values for the $d + d \to n + {}^3$He reaction at $E_d = 3$ MeV predicted by AV18, N3LO, CD Bonn, CD Bonn + Δ, and INOY04 models are 0.133, 0.159, 0.164, 0.185, and 0.219, respectively. Thus, the QSF correlates with both $3N$ binding energy and $P_D(d)$, increasing when the former increases and/or the latter decreases.

III. SUMMARY

In summary, we performed exact four-particle calculations of $d + d \to p + {}^3$H and $d + d \to n + {}^3$He reactions with several realistic NN potentials. Energy dependence of the differential cross section and spin observables was studied below the three-body breakup threshold. Correlations of the predictions with $3N$ binding energy and deuteron D-state probability $P_D(d)$ were observed. The INOY04 potential that fits both ^{3}He and ^{3}H experimental binding energies and has the smallest $P_D(d) = 3.60\%$ among all realistic potentials accounts well for the experimental data with only few discrepancies, for example, the one in the deuteron-tensor-analyzing power T_{20}. Some data suggest that even smaller $P_D(d)$ would be preferred. We also predict the QSF in the $d + d \to n + {}^3$He reaction to be only up to 25% smaller than the one in $d + d \to p + {}^3$H; the d-d fusion with spin-aligned deuterons seems to be significantly suppressed at few MeV but not in the keV regime.

[1] A. Deltuva and A. C. Fonseca, Phys. Rev. C **75**, 014005 (2007).

[2] A. Deltuva and A. C. Fonseca, Phys. Rev. C **76**, 021001(R) (2007).

[3] P. Grassberger and W. Sandhas, Nucl. Phys. B **2**, 181 (1967); E. O. Alt, P. Grassberger, and W. Sandhas, JINR Report No. E4-6688 (1972).

[4] J. M. Blair, G. Freier, E. Lampi, W. Sleator, and J. H. Williams, Phys. Rev. **74**, 1599 (1948).

[5] G. T. Hunter and H. T. Richards, Phys. Rev. **76**, 1445 (1949).

[6] W. Grüebler, V. König, P. A. Schmelzbach, R. Risler, R. E. White, and P. Marmier, Nucl. Phys. A **193**, 129 (1972).

[7] W. Grüebler, V. König, P. A. Schmelzbach, B. Jenny, and J. Vybiral, Nucl. Phys. A **369**, 381 (1981).

[8] L. J. Dries, H. W. Clark, R. Detomo, and T. R. Donoghue, Phys. Lett. B **80**, 176 (1979).

[9] R. A. Hardekopf, R. L. Walter, and T. B. Clegg, Phys. Rev. Lett. **28**, 760 (1972).

[10] P. Lisowski, R. Walter, C. Busch, and T. Clegg, Nucl. Phys. A **242**, 298 (1975).

[11] C. D. Roper, T. B. Clegg, J. D. Dunham, A. J. Mendez, W. Tornow, and R. L. Walter, Few-Body Syst. **47**, 177 (2010).

[12] R. M. Kulsrud, H. P. Furth, E. J. Valeo, and M. Goldhaber, Phys. Rev. Lett. **49**, 1248 (1982).

[13] H. M. Hofmann and D. Fick, Phys. Rev. Lett. **52**, 2038 (1984).

[14] O. A. Yakubovsky, Yad. Fiz. **5**, 1312 (1967) [Sov. J. Nucl. Phys. **5**, 937 (1967)].

[15] J. R. Taylor, Nuovo Cimento B **23**, 313 (1974); M. D. Semon and J. R. Taylor, Nuovo Cimento A **26**, 48 (1975).
[16] A. Deltuva, A. C. Fonseca, and P. U. Sauer, Phys. Rev. C **71**, 054005 (2005); **72**, 054004 (2005).
[17] A. Deltuva and A. C. Fonseca, Phys. Rev. Lett. **98**, 162502 (2007).
[18] E. O. Alt and W. Sandhas, Phys. Rev. C **21**, 1733 (1980).
[19] R. B. Wiringa, V. G. J. Stoks, and R. Schiavilla, Phys. Rev. C **51**, 38 (1995).
[20] R. Machleidt, Phys. Rev. C **63**, 024001 (2001).
[21] P. Doleschall, Phys. Rev. C **69**, 054001 (2004).
[22] D. R. Entem and R. Machleidt, Phys. Rev. C **68**, 041001(R) (2003).
[23] A. Deltuva, R. Machleidt, and P. U. Sauer, Phys. Rev. C **68**, 024005 (2003).
[24] A. Deltuva, A. C. Fonseca, and P. U. Sauer, Phys. Lett. B **660**, 471 (2008).
[25] H. M. Hofmann and G. M. Hale, Phys. Rev. C **77**, 044002 (2008).
[26] H. Paetz gen. Schieck (private communication).
[27] J.-P. Didelez (private communication).